Study on the Preparation of TiO_2-SiO_2 Composites from Rice Husk Ash

Yu Liang, Xiaoyu Ma*, Suping Cui, Zhihong Wang, Yali Wang
College of Materials Science and Engineering, Beijing University of Technology, China

Abstract: In this paper, TiO_2-SiO_2 composites with different SiO_2 contents were prepared by coprecipitation method using rice husk ash as raw material. The effects of the concentration of alkaline leaching solution and reaction temperature on the extraction rate of SiO_2 from rice husk ash were investigated. The optimum formation conditions of TiO_2-SiO_2 composites were explored, and the microstructure and properties of the composites were analyzed. The experimental results showed that the extraction rate of SiO_2 from rice husk ash reaches the maximum when the concentration of alkaline leaching solution is 1.5 mol/L and the reaction temperature is 90℃. When the pH value is 7, the TiO_2-SiO_2 composites can achieve the optimum formation condition. TiO_2-SiO_2 composites are composed of approximately spherical particles with obvious pore structure of the surface and piling up in fluffy state. The Si atoms enter the crystal structure of TiO_2 with Ti-O-Si bonds connected to Ti atoms, which inhibits the growth of TiO_2 grains and leads to the increase of the transition temperature of TiO_2 from anatase to rutile.

1 Introduction

In recent years, nanoscale TiO_2 has been widely used in the fields of seawater desalination, photocatalysis and solar cells for its high weather ability and excellent optical and mechanical properties[1-3].However, the pure TiO_2 has many defects such as higher price, smaller specific surface area and weaker acid, leading thatthe development demand of many fields is limited[4]. Therefore, in order to overcome these defects and improve the physical and chemical properties of TiO_2, it is usually combined with SiO_2, Fe_2O_3or CeO_2 to form composite oxide materials with low density and high porosity[5-6]. Among them, SiO_2 has high bonding strength, large specific surface area and good thermal stability[7],in addition, TiO_2-SiO_2 composites after adding SiO_2 can have excellent properties of TiO_2 and SiO_2 at the same time[8]. Therefore, TiO_2-SiO_2 composites have become the focus of research. At present, most laboratories apply sol-gel or coprecipitation to synthesis TiO_2-SiO_2 composites that were made from titanium butoxide and tetraethyl orthosilicate[9-10].However, the hydrolysis rate of ester organic compounds is faster, the experimental conditions are demanding, and the price of themare relatively high, so the industrial production of TiO_2-SiO_2 composites are limited in some extent. It is found that there are a lot of amorphous SiO_2 in rice husk ash from agricultural waste[11],and the alkaline solution of SiO_2 is easy to react with $Ti(SO_4)_2$ solution[12]. Accordingly, TiO_2-SiO_2 composites can be prepared by cheap rice husk ash and $Ti(SO_4)_2$ as precursors, which can not only rationalize the utilization of agricultural waste, but also protect the environment and create higher commercial value[13].

In this paper, cheap and readily available rice husk ash and $Ti(SO_4)_2$ were used as silicon source and titanium source respectively to prepare TiO_2-SiO_2 composites, which were applied to coprecipitation method to adjust the pH value by the ammonia titration. The

Corresponding author: Xiaoyu Ma. Email: maxiaoyu@bjut.edu.cn

microstructure and properties of TiO_2-SiO_2 composites were studied by means of BET, SEM, FT-IR and XRD.

2 Experiment

2.1 Preparation of TiO_2-SiO_2 Composites

First, the rice husk ash and alkaline leaching solution are heated and mixed in a flask, and the sodium silicate solution is obtained through filtration. Then add appropriate concentration of $Ti(SO_4)_2$ solution slowly and regulate pH value through ammonia water in it. Last, TiO_2-SiO_2 composites with different SiO_2 contents were obtained after filtration, drying and calcining in muffle furnace (FR-1236). The prepared samples were represented by TiO_2-SiO_2(x), where x was the content of SiO_2 in TiO_2-SiO_2 composites.

2.2 Characterization of TiO_2-SiO_2 Composites

Micromeritics's TriStar 3020 high speed automatic specific surface area and pore analyzer was used for the specific surface area and pore structure analysis (BET) of the TiO_2-SiO_2 composites. The specific surface area is calculated by Brunauer-Emmett-Teller and the pore size distribution is obtained by measuring the N_2 desorption isotherm and calculating it by Barrett-Joyner-Halenda (BJH); The crystal structure and morphology of TiO_2-SiO_2 composites were analyzed by XRD-7000 X-ray diffraction analyzer produced by Shimadzu Corporation. Cu is the target. Ka is the radiation source. The tube voltage is 40KV and the scanning range is 10~70 degrees; The FTIR-8400S infrared spectrometer was used for analyzing the TiO_2-SiO_2 composites by Fourier infrared spectroscopy (FT-IR). The sample was dried, ground and pressed test and the test range was 400-1400cm^{-1}; The QUANTA 600F scanning electron microscope (SEM) of FEI company was used for analyzing the microstructure of the surface of TiO_2-SiO_2 composites.

3 Discussion of results

3.1 The influence factors on the extraction of SiO_2 from rice husk ash

The composition of rice husk ash showed that the content of SiO_2 in rice husk ash reached 37.5% and the rests are carbon and a small amount of metal[8]. Its component analysis results are shown in Table 1

3.1.1 The effect of concentration of alkaline leaching solution on extraction rate of rice hull ash

The 20.0g rice husk ash where the mass of SiO_2 is about 7.5g from the table 1 was reacted with the 200ml alkaline leaching solution whose OH^- concentration is 0.5~4mol/L respectively. The relationship between the extraction rate of rice husk ash and OH^- concentration is shown in Fig. 1. With the increase of OH^- concentration, the extraction rate of rice husk ash is becoming larger and larger. When the concentration of OH^- is 1.5mol/L, the reaction of SiO_2 in rice husk ash and alkaline leaching solution are gradually complete, and the extraction rate of rice husk ash reaches the maximum. As the concentration of OH^- in the alkaline leaching solution continues to increase, the excess OH^- may react with the metal in rice husk ash, the residual sediment increases and the extraction rate of rice husk ash begins to decreases. So the optimum concentration of OH^- in the alkaline leaching solution is 1.5 mol/L. Fitting the curve before the extraction rate of rice husk ash reaching the maximum value, a straight line equation can be obtained, y=41.26667+37.4x. Verifying the extraction rate of SiO_2 in rice husk ash with alkaline leaching solution that the concentration of is 1.2 mol/L is 86%, which is approximated to 86.15% that is calculated. The more OH^- in alkaline leaching solution, the more reaction amount to SiO_2. Accordingly, there is a linear relationship between the extraction rate of SiO_2 before reaching the maximum value and the concentration of OH^- in alkaline leaching solution.

Table 1 the main components of rice husk ash

Component	SiO_2	K_2O	P_2O_5	CaO	MgO	SO_3	Al_2O_3	C
Content（%）	37.5	1.8	1.2	0.6	0.5	0.4	0.2	57.8

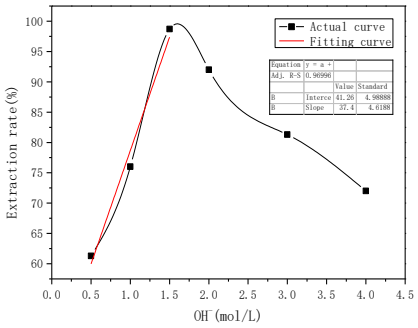

Fig. 1 The relationship between the extraction rate of rice husk ash and OH^- concentration in alkaline leaching solution

3.1.2 The effect of reaction temperature on extraction rate of rice hull ash

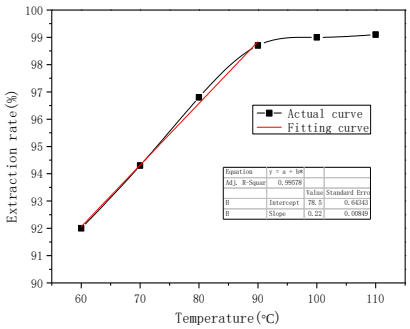

Fig. 2 The relationship between the extraction rate of rice husk ash and reaction temperature

In order to fully extract SiO_2 from rice husk ash, the relationship between the extraction rate of rice husk ash and the reaction temperature was investigated, as shown in Fig. 2. With the increase of reaction temperature, the extraction rate of rice husk ash increases gradually. When the temperature rises to 90℃, the extraction rate of rice husk ash reaches 98.7%. As the temperature continues to raise, the extraction rate of rice husk ash tends to be gentle. The fitting analysis of the curve before 90℃ can be seen that the extraction rate of rice husk ash is linear with temperature. The equation is y=78+0.226x. Verifying the extraction rate of SiO_2 in rice husk ash at 60℃ and 75℃ are 92.65% and 95% respectively, which are approximated to 92.69% and 94.95%, both of which are calculated. Therefore, when the reaction temperature is less than 90℃, the extraction rate of rice husk ash increases linearly with the increase of reaction temperature. It can also be proved that the reaction between rice husk ash and alkaline leaching solution accords with the first order reaction of kinetic equation.

3.2 The characterization of TiO_2-SiO_2composites materials

3.2.1 The effect of pH value on the generation of TiO_2 and SiO_2

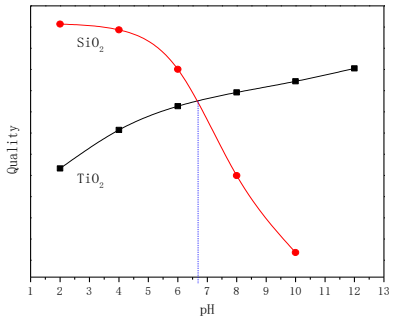

Fig. 3 The effect of pH value on the generation of TiO_2 and SiO_2

The pH value is a key factor affecting the generation of TiO_2 and SiO_2. By adjusting the pH of the solution, it can not only determine the ratio of TiO_2 to SiO_2 in TiO_2-SiO_2 composites, but also obtain the optimal generation condition of TiO_2-SiO_2 composites. As shown in Fig. 3, when pH is 10, white silica sol begins to form in sodium silicate solution. With the decrease of pH, more and more white colloid forms in the solution, because of the H^+ first reacting with SiO_3^{2-} in the solution[13],which indicates that the quality of SiO_2 is bigger and bigger. When the pH of solution is 2, the mass of SiO_2 reaches the maximum value, which indicates that SiO_2 is more suitable for generation in acid solution. When the pH value is 2, white titanic acid begins to be produced in $Ti(SO_4)_2$ solution. As the pH increases, more and more white precipitate generates in $Ti(SO_4)_2$ solution, which indicates that the amount of TiO_2 is increasing. Considering the optimum generation amount of two oxides, It can be determined that the optimum pH value of TiO_2-SiO_2 composites is 7.

3.2.2 Analysis of specific surface area and pore structure of TiO_2-SiO_2 composites

Table. 2 Specific surface area and pore distribution of TiO_2-SiO_2 composites with different SiO_2 content

Sample	S_{BET}（m^2/g）	Pore volume（cm^3/g）	Pore diameter（nm）
TiO_2	145.7	0.33	9.7
TiO_2-SiO_2(0.2)	253.6	0.62	7.9
TiO_2-SiO_2(0.5)	355.5	0.65	7.6
TiO_2-SiO_2(0.8)	413.9	0.64	7.4
SiO_2	463.9	0.70	6.5

In order to investigate the effect of SiO_2 content on the surface structure of TiO_2-SiO_2 composites, the specific surface area and pore structure of the composites were analyzed in this paper, as shown in Table 2.

It can be seen from the table that the specific surface area and pore volume of pure TiO_2 are the smallest. With the increase of SiO_2 content, the specific surface area of TiO_2-SiO_2 composites is larger and larger, and the pore volume also increases gradually. In the TiO_2-SiO_2(0.8), the content of SiO_2 is high and Si atoms affect the formation of Ti atoms, resulting in the complete collapse of the framework of TiO_2. Therefore, the pore volume decreases. When the content of SiO_2 is 100%, the specific surface area and pore volume reach the maximum value. In the TiO_2-SiO_2 composites, the pores of SiO_2 particles are occupied by the TiO_2 powders, so the specific surface area and pore volume decrease rapidly when the content of TiO_2 powders are high[14].

3.2.3 Analysis of SEM test results

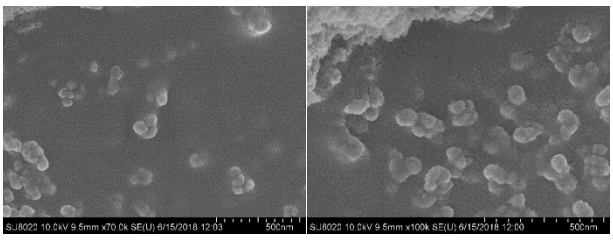

(a) (b)

Fig. 4 Microstructural diagrams of TiO_2-SiO_2(0.5) composites
(a) Under the condition of 70,000 times; (b) Under the condition of 100,000 times

Fig. 4 are SEM diagrams of TiO_2-SiO_2(0.5) composites under the condition of 70,000 times and 100,000 times. It can be seen from the diagram that the TiO_2-SiO_2 composites are made up of nearly spherical particles, and the particle size is about 40~50nm. The distribution of TiO_2-SiO_2 composites is more dispersed, mostly consisting of three or four spherical particles with different sizes. It shows that SiO_2 and TiO_2 are combined with stable chemical bonds.

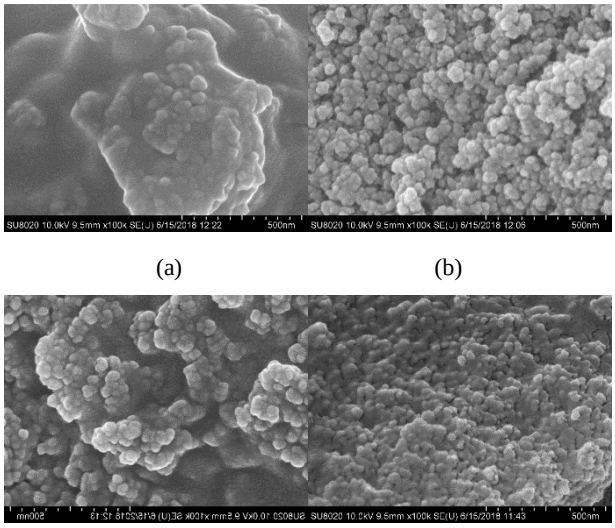

(a) (b)

(c) (d)

Fig. 5 SEM diagrams of TiO_2-SiO_2 composites with different SiO_2 content
(a) Pure TiO_2; (b) TiO_2-SiO_2(0.2);
(c) TiO_2-SiO_2(0.5); (d) TiO_2-SiO_2(0.8)

Fig. 5 are SEM diagrams of TiO_2-SiO_2 composites with different SiO_2 content at the magnification of 100 thousand times. As is shown in the Fig. 5(a), pure TiO_2 particles are large, the surface is smooth and the internal pore structure is not obvious, so the specific surface area and pore volume are relatively low. With the addition of SiO_2, the particles on the surface of TiO_2-SiO_2 composites decrease and uniform gradually, the surface smoothness reduces, and the pore structure becomes more and more obvious. When the content of SiO_2 reaches 80%, the surface of the composites exhibit melting shape, which exists a large number of pore structures, and the fine and uniform particles are fluffy in the surface. Therefore, the specific surface area and pore volume are relatively higher, which are in agreement with the analysis results of Table 2.

3.2.4 FT-IR analysis of TiO_2-SiO_2 Composites

In order to determine the form of SiO_2 and TiO_2 in

TiO_2-SiO_2 composites, FT-IR tests were performed on three oxides of SiO_2, TiO_2 and TiO_2-SiO_2(0.5) respectively, as shown in Fig. 6.

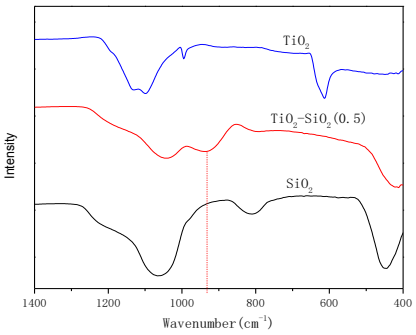

Fig. 6 the FT-IR diagram of three oxides

As can be seen from Fig. 6, the three oxides have different infrared absorption peaks at different positions, of which the absorption peak at 610cm^{-1} belongs to the stretching vibration of the Ti-O-Ti bond, and the absorption peak at 445cm^{-1}, 810cm^{-1}and 1066cm^{-1} belong to the stretching vibration of the Si-O-Si bond[15]. It has been proved that the infrared absorption peak of 920~970cm^{-1} is the characteristic absorption peak of the Ti-O-Si bond[16]. The infrared characteristic absorption peak of Ti-O-Si bond can be detected clearly in TiO_2-SiO_2 composites, while the infrared characteristic absorption peak of Ti-O-Ti bond disappears. It proves that the combination of TiO_2 and SiO_2 in the form of chemical bonds, rather than simple physical mixing, which is in line with the analysis results of SEM. During the formation of TiO_2-SiO_2composites, Si atoms enter the network framework of TiO_2 in the form of substituted cations and connect with Ti atoms in the form of Ti-O-Si bond. As the Ti atomic radius (0.064nm) is larger than the radius of the Si atom (0.041nm), and the length of Ti-O bond (0.179nm) is longer than the length of Si-O bond (0.159nm), which cause the growth of the TiO_2 crystal being inhibited and the grain size becomes smaller[17]. Therefore, The Ti atom transforms from octahedral coordination to tetrahedral coordination gradually[18].

3.2.5 Analysis of XRD test results

In order to study the effect of SiO_2 content and calcination temperature on the crystal structure of TiO_2, different kinds of samples were tested by XRD respectively. The results are shown in Fig. 7.

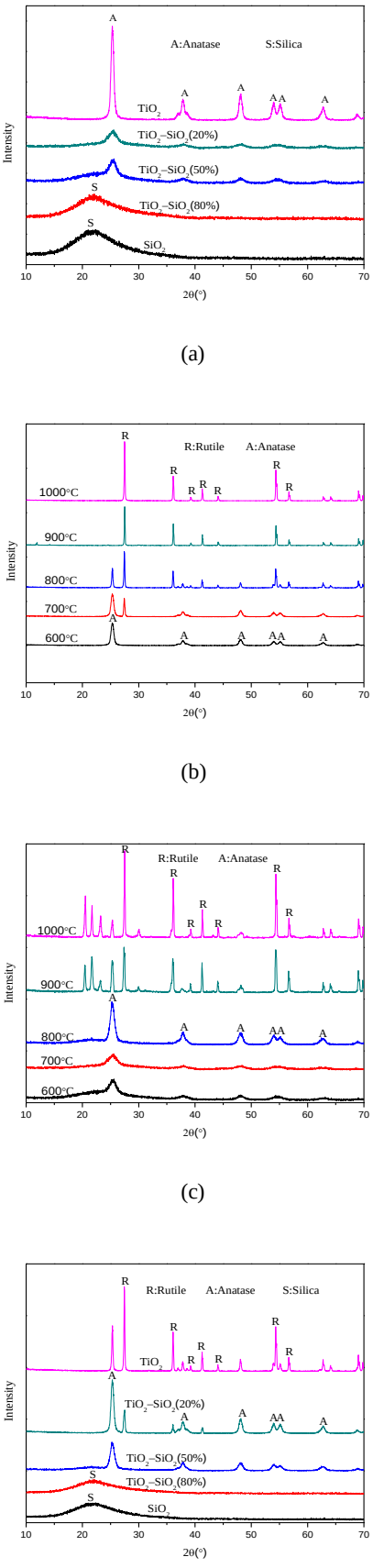

Fig. 7 XRD diagrams under different conditions

(a) TiO_2-SiO_2(x) at 600℃; (b) Pure TiO_2 at 600~1000℃
(c) TiO_2-SiO_2(0.5) at 600~1000℃; (d) TiO_2-SiO_2(x) at 800℃

XRD test chart of TiO_2-SiO_2 composites with different SiO_2 contents at 600℃ are shown in Fig. 7(a). When the content of SiO_2 is less than 20%, the diffraction peak of anataseTiO_2 exists only in TiO_2-SiO_2 composites, and the peak value is highest and the width is narrowest. With the addition of SiO_2, the characteristic peaks of anataseTiO_2 gradually generalize and the peaks value gradually decrease, but the characteristic peak of SiO_2 gradually becomes obvious. When the content of SiO_2 is higher than 50%, the characteristic peaks of anataseTiO_2 disappear, and a steamed bread shaped peak is found near 22.5 degrees, indicating that the TiO_2-SiO_2composites was mainly in the form of amorphous SiO_2[19]. Therefore, as SiO_2 content increases, the crystallinity of TiO_2 in TiO_2-SiO_2 composites decreases gradually.

Fig. 7(b) and Fig. 7(c) are XRD test results of pure TiO_2 and TiO_2-SiO_2(0.5) composites at 600~1000 temperature. As can be seen from Fig. 7(b), when the temperature is 700℃, the pure TiO_2 begins to appear weak rutile characteristic diffraction peaks, indicating that part of the anataseTiO_2 changes to the rutile structure gradually. When the temperature rises to 900℃, the characteristic diffraction peak of anatase is disappeared, and TiO_2 transforms into rutile structure completely. As is shown in Fig. 7(c), compared with pure TiO_2, the phase transformation temperature of TiO_2-SiO_2(0.5) composites is higher. When the temperature rises to 900℃, the rutile characteristic diffraction peak appears. Therefore, the addition of SiO_2 increases the transition temperature of TiO_2 from anatase to rutile and also improves its thermal stability.

Fig. 7(d) are the XRD test result of TiO_2-SiO_2 composites with different SiO_2 contents at 800℃. Pure TiO_2 has the strongest rutile characteristic peak, the width of which is the narrowest. With the increase of SiO_2 content, the diffraction peaks of rutile decrease gradually and become wider and wider. When the content of SiO_2 is higher than 50%, the characteristic diffraction peaks of rutile disappear and the characteristic diffraction peaks of anatase become generalized. The characteristic diffraction peaks of TiO_2 in TiO_2-SiO_2 composites disappeared gradually with the increase of SiO_2 content. Some studies have shown that the transformation of TiO_2 from anatase to rutile is caused by lattice stress and cell volume[20].The smaller the cell volume is, the higher the transition temperature is. Accordingly, with the increase of SiO_2 content, it can be speculated that the grain size of TiO_2-SiO_2 composites decreases gradually, which is consistent with the results of SEM and FT-IR.

4 Conclusion

1. Using rice husk ash as silicon source and $Ti(SO_4)_2$ as titanium source, the TiO_2-SiO_2 composites with different SiO_2 content can be prepared by coprecipitation method. When the concentration of OH^- in alkaline leaching solution is 1.5 mol/L and the reaction temperature is 90℃, the extraction of SiO_2 from rice husk ash reaches the maximum value. SiO_2 and TiO_2 can reach the optimal amount of generation by adjusting pH to 7 with ammonia water.

2. Most of the TiO_2-SiO_2 composites are composed of 3~4 approximately spherical particles, which accumulate in a fluffy state. The surface of the composites are rough and the pore structure is obvious. With the increase of SiO_2 content, the specific surface area and pore volume increased gradually.

3. During the formation of TiO_2-SiO_2 composites, Si atoms enter the crystal structure of TiO_2 in the form of substituted cations and connect to Ti atoms in the form of Ti-O-Si bond, which inhibits the crystal growth of TiO_2, makes the grain size of TiO_2 smaller, and eventually leads to the transition temperature of TiO_2 in TiO_2-SiO_2 composites from anatase to rutile increases. Besides, as theSiO_2 content increases, the crystal transition temperature increases gradually.

Acknowledgement

This study has been supported by the The National Natural Science Foundation of China (51502008); National Key R&D Plan (2017YFB0310802).

Reference

[1] K. Hashimoto, H. Irie, A. Fujishima. J. JPN J APPL PHYS,. **44**, 8269-8285 (2014).
[2] R. Wang, K. Hashimoto, A. Fujishima, et al. J. Adv. Mater, **10**, 135-138 (2010).
[3] P. Zhang, F Y. Lv. J. ENERGY, **82**, 1068-1087 (2015).

[4] S. Cao, N. Yao, K L. Yeung. J. J SOL-GEL SCI TECHN, **46**, 323-333 (2008).

[5] W. Dong, Y. Sun, C W. Lee, et al. J. J AM CHEM SOC, **129**, 13894-13904 (2007).

[6] L. Pinho, M J. Mosquera. J. APPL CATAL B-ENVIRON, **134-135**, 205-221 (2013).

[7] M A L. Vargas, M. Casanova, A. Trovarelli, et al. J. APPL CATAL B-ENVIRON, **75**, 303-311 (2007).

[8] Y. Liu. D. JILIN U, (2013).

[9] J. Krzakroś, J. Filipiak, C. Pezowicz, et al. J. Acta Bioeng Biomech, , **11**, 21 (2009).

[10] C. Hu, Y. Tang, Z. Jiang, et al. J. APPL CATAL A-GEN, **253**, 389-396 (2003).

[11] D. Ouyang, K. Chen. J. Journal of Chinese Electron Microscopy Society, **22**, 390-394 (2003).

[12]Y. Cheng. D. JILIN U, (2017).

[13] Y. Liu. D. JILIN U,(2015).

[14] F Y. Sun, J H. Lin, K F. Ren, et al. J. B CHIN CERAM SOC, **35**, 870-874 (2016).

[15] X. Gao, I E. Wachs. J. CATAL TODAY, **51**, 233-254 (1999).

[16] S. Zhu, D. Zhang, X. Zhang, et al. J. MICROPOR MESOPOR MAT, **126**, 20-25 (2009).

[17] C F. Song, K L. Meng, P. Yang, et al. J. THIN SOLID FILMS, **413**, 155-159 (2002).

[18] J B. Miller, E I. Ko. J. J CATAL, **159**, 58–68 (1999).

[19] P C. Arroyomartínez, N A. Sánchezflores, M E, Villafuertecastrejón, et al. J. J.braz.chem.soc, **29**, 1 (2018).

[20] L Y. Wang, Y P. Sun, B S. Xu. J. J MATER SCI, **43**, 1979-1986 (2008).